DOI:
10.1016/j.ijpharm.2016.08.012

Document Version
Peer reviewed version

Controlled drug release from lung-targeted nanocarriers via chemically mediated shell permeabilisation

Hanpeng Chen, Arcadia Woods, Ben Forbes, Stuart Jones*

Institute of Pharmaceutical Science, Faculty of Life Sciences & Medicine, Franklin-Wilkins Building, King's College London, 150 Stamford Street, London SE1 9NH, UK.

*Corresponding author. Dr. S. A. Jones. King's College London, Faculty of Life Sciences & Medicine, Institute of Pharmaceutical Science, Franklin-Wilkins Building, 150 Stamford Street, London, SE1 9NH. Tel: +44 (0)207 848 4843. Fax: +44 (0)207 848 4800. E-mail:stuart.jones@kcl.ac.uk

Abstract

Nanocarriers can aid therapeutic agent administration to the lung, but controlling drug delivery from these systems after deposition in the airways can be problematic. The aim of this study was to evaluate if chemically mediated shell permeabilisation could help manipulate the rate and extent of nanocarrier drug release. Rifampicin was loaded into lipid shell (loading efficiency 41.0 ± 11.4%, size 50 nm) and polymer shell nanocarriers (loading efficiency 25.9 ± 2.3%, size 250 nm). The drug release at pH 7.4 (lung epithelial pH) and 4.2 (macrophage endosomal pH) with and without the chemical permeabilisers (Pluronic L62D - lipid nanocarriers; H^+- polymer nanocarriers) was then tested. At pH 7.4 the presence of the permeabilisers increased nanocarrier drug release rate (from 3.2 µg/h to 6.8 µg/h for lipid shell nanocarriers, 2.3 µg/h to 3.4 µg/h for polymer shell nanocarriers) and drug release extent (from 50% to 80% for lipid shell nanocarriers, from 45% to 76% for polymer shell nanocarriers). These effects were accompanied by lipid nanocarrier distension (from 50 to 240 nm) and polymer shell hydrolysis. At pH 4.2 the polymer nanocarriers did not respond to the permeabiliser, but the lipid nanocarrier maintained a robust drug release enhancement response and hence they demonstrated that manipulation of controlled drug release of lung-targeted nanocarriers was possible through chemically mediated shell permeabilisation.

Key words: Lipid nanoparticles; polymer nanoparticles, inhaled drug delivery, rifampicin, poly(vinyl alcohol), controlled drug release; dissolution.

1. Introduction

The incorporation of drugs into nanocarriers can enhance their delivery by improving the agents chemical stability, water solubility and *in-vivo* clearance rates (Parveen et al., 2012; Peer et al., 2007). However, for nanocarriers to realise these benefits they must be able to hold an appropriate amount of an active agent and control its release at the site of delivery. The large surface area to volume ratio of nanocarriers can be problematic when attempting to control drug release because it renders them highly sensitive to interactions with the bodily fluids into which they are delivered. As a consequence, nanocarrier systems have a tendency to display an immediate release of their drug payloads (Natarajan et al., 2014). If the initial release rate is rapid and it liberates a significant portion of drug in a short period then this can negate the potential of the nanocarriers to protect their drug payloads from chemical instability and rapid *in-vivo* clearance (Danhier et al., 2009; Janes et al., 2001).

Improving the affinity of the drug for the carrier, e.g., by forming ion-pairs in the carrier matrix (Holmkvist et al., 2016; Pinkerton et al., 2012), can reduce the immediate release effect experienced by some nanocarrier systems and in some cases it can act to sustain drug release over several days (Mukherjee et al., 2008). However, paradoxically, such a slow release can create another problem, incomplete drug liberation. For therapeutic use, nanocarriers must release their payload to produce the target pharmacokinetic profile in a timeframe that complements carrier clearance dynamics. The ideal scenario is to use a system which allows strong retention of the drug during formulation storage and complete liberation upon delivery to provide the desired duration of drug action. This is very difficult to achieve inherently and there is a need to develop active release strategies that will control drug delivery from nanocarriers upon administration.

Nanocarriers that change their form in response to an external stimuli provide a potential solution to poor drug release by nanocarriers (Mura et al., 2013). Active release can be induced in response to the biological environment upon administration or can be achieved using specific chemical or physical stimuli (Ganta et al., 2008). In respiratory drug delivery, nanocarriers can be co-formulated with trigger agents such that the exogenous chemical agent is available to modify drug release after deposition in the airways of the lung. Because inhaled products employ micron-sized particles to facilitate deposition (Wang et al., 2012), the nanocarrier and the agent used to control drug release can be immobilised in a microparticle formulation. Upon inhalation, the microparticle will deposit in the airways and

dissolve in the liquid-limited mucosal surface such that the chemical trigger the nanocarrier mix at the point of delivery.

The aim of this study was to assess whether the co-administration of nanocarrier shell permeabilisers is a practicable strategy to control drug release from nanocarriers. Two nanocarriers with different shell properties were investigated. These were a polymeric shelled nanocarrier, constructed with a lipid benzyl benzoate core, a phospholipid intermediate layer and an outer poly(vinyl alcohol) (PVA) shell and a lipidic shelled nanocarrier, which contained a triglyceride core and a semi-solid phosphatidylcholine / PEG hydroxystearate shell. Both the nanocarriers have been shown to be biocompatible with lung airway cells (Chana et al., 2015; Madlova et al., 2009) and their safety has been assessed by acute lung toxicity testing in mice (Jones et al., 2014). The shell permeabiliser for the lipid nanocarrier was a Pluronic surfactant, whereas for the polymer nanocarrier an acidic environment was used to hydrolyse the polymer and modify shell permeability. Both these shell permeabilisers have been shown to be biocompatible with lung airway cells in previous work (Chana et al., 2015). As there is a need to localise anti-tuberculosis (TB) drugs in the respiratory system for extended periods of time (Sosnik et al., 2010) and previous work had shown burst release was a problem for these agents (Ohashi et al., 2009; Pandey et al., 2003), rifampicin was selected as the model agent for the study. Previous work with rifampicin has shown that this agent is chemically unstable in water and therefore nanocarriers could be particularly beneficial for this agent (Singh et al., 2013). To understand better how the model drug would be released from the nanocarriers two pH conditions, 7.4 and 4.2 were used in the drug release studies. These two particular pHs were selected as they are relevant to environments encountered in the lungs, i.e., they mimicked the pH of the airways and lysosomal compartments of alveolar macrophages, respectively (Mindell, 2012). The investigation included effect of the chemical triggers on the rate and extent of drug release, plus explored how modified release was achieved by applying analytical tests to probe nanocarrier shell transformations.

2. Materials and methods

2.1. Materials

Medium chain triglycerides (Labrafac® lipophile 1349), purified phosphatidylcholine (> 90 %) from soybean lecithin (Epikuron® 200) and PEG 15 hydroxystearate (Solutol® HS15) were kindly supplied by Gattefossé S.A. (Saint- Preist, France), Cargill GmbH (Germany), and BASF (Ludwigshafen, Germany), respectively. Pluronic®L62D was sourced from BASF

(New Jersey, USA). Poloxamer 188was from BASF (Ludwigshafen, Germany) and Epikuron phospholipid was from Cargill GmbH (Germany). Sodium chloride, sodium hydroxide, citric acid, sodium citrate, poly(vinyl acetate) (Mw 12800), benzyl benzoate and rifampicin (≥ 97%, HPLC) were purchased from Sigma Aldrich (Gillingham, UK). High performance liquid chromatography (HPLC) grade water, ethanol and methanol were obtained from Fischer Scientific (Leicestershire, UK).

2.2. Fabrication of lipid shell nanocarriers

The lipid shell nanocarriers were manufactured via precipitation from a stable emulsion following repeated phase inversion, as described by Heurtault et al (Heurtault et al., 2002). Medium chain triglycerides (17% w/w), phosphatidylcholine (1.75% w/w), PEG hydroxystearate (17% w/w) and a 3% w/v sodium chloride aqueous solution (64.25% w/w) were mixed at room temperature and then heated to 85°C at a rate of 4°C per minute, with continuous magnetic stirring. The mixture was then allowed to cool to 60°C. The temperature of the mixture was cycled between 60°C and 85°C a total of three times. Within this temperature range phase inversion occurred with an oil-in-water emulsion being converted to a water-in-oil emulsion. Following the final heating cycle, the emulsion was allowed to cool to 72°C, at which point 25 mL of ice-cold water was added, causing nanocarrier generation. The suspension was stirred for 5 min and then made up to a final volume of 50 mL using deionised water. The lipid shell nanocarrier suspensions were purified of excess excipients and larger particulate matter via centrifugation (Beckman L8-80 ultracentrifuge, Beckman Coulter, Buckinghamshire, UK) at 110,000 *g*, 25°C for 1 h. The suspension was separated into three distinct layers; an upper gel like layer, a middle lipid shell nanocarrier suspension layer, and a bottom sediment layer. The purified suspension layer was used for further experimental work.

2.3. Fabrication of polymer shell nanocarriers

The synthesis of PVA used to produce the polymer shell nanocarriers was based on direct saponification method. PVA32% hydrolysis was produced from a poly(vinyl acetate) with the optimal reaction conditions which had previously been published (Chana et al., 2008). The percentage hydrolysis of the PVA polymer was determined by nuclear magnetic resonance (NMR) analysis and calculated according to the previously detailed (Chana et al., 2008).

The polymer shell nanocarriers were fabricated by nanoprecipitation (Madlova et al., 2009). Briefly citrate buffer was prepared by adding 40 mL of 0.1 M citric acid solution to 60 mL of 0.1 M sodium citrate solution and adjusted to achieve a pH of 4.8. Poloxamer 188 (0.5 % w/v) was added to citrate buffer and made up to a volume of 100 mL. Methanol: water with a ratio of 9:1 v/v was used as organic solvent. A mixture of 50 mg PVA and 75 mg of Epikuron phospholipid was dissolved in 5 mL and 10 mL of organic solvent respectively. A 0.33 mL aliquot of benzyl benzoate was added to the methanol/water mixture to complete the organic dispersing phase. To fabricate the nanocarriers, the aqueous phase (30 mL) was homogenized at 5000 rpm for 2 min and then 15 mL of the organic phase was added drop-wise, at a speed of 8 mm/min, using a syringe pump. The homogenization process was continued for 10 minutes. The suspension produced was transferred to the fume hood and left to stir 20 h to remove the organic solvent. The suspension was centrifuged at 4000 rcf for 5 min at 20 °C to remove large particle contamination.

2.4. Nanocarrier characterization

The nanocarrier size was analysed using photon correlation spectroscopy (PCS) (Zetasizer Nano, Malvern Instruments, Worcestershire, UK). All measurements were carried out at a scattering angle of 173° using water as the dispersant (refractive index 1.33, viscosity 0.8872 cP at 37°C). Each measurement comprised 10-14 runs and was performed in triplicate for each sample. Mean diameters obtained from the size-intensity frequency distributions were reported. To investigate the effect of suspension concentration on the accuracy of the size measurement, and to determine the absolute carrier diameter, analyses were performed on nanocarrier suspensions serially diluted with HPLC grade water (n = 3). Mean diameter was plotted against suspension concentration, and the y-axis intercept following linear regression analysis was determined as the absolute diameter. The zeta potential of the nanocarrier was determined by measurement of their electrophoretic mobility (Zetasizer Nano, Malvern Instruments, Worcestershire, UK). Samples were analysed following dilution with HPLC grade water. Each measurement comprised between 50 to 100 runs and was performed in triplicate at 37°C.In order to determine the solid content (mg/mL) of the purified nanocarrier suspensions, 0.5 mL aliquots were transferred to Amicon centrifuge tubes and spun for 30 min. The nanocarrier collection chambers were removed from the tubes and dried in a fume hood until a constant mass of particles collected from the centrifugation process was recorded.

2.5. HPLC analysis of rifampicin

HPLC quantification of rifampicin was performed using a Jasco HPLC pump and a dual absorbance detector. A reversed-phase C18 column was used (Phenomenex Gemini 5µm C18, 250×4.60 mm). UV detection was performed at 335 nm. The mobile phase consisted of acetonitrile: PBS buffer (40: 60 % v/v) pH 7.4 at a rate of 1 mL/min. A 20 µL sample was injected onto the column for all the analysed samples. Each sample was quantified by reference to a calibration curve with a range of 0.1-0.002 mg/mL. The linearity (R^2> 0.999), the average intra-day precision (1.8 %), inter-day precision (2.4 %), limit of detection and limit of quantification (2.5 and 8.4 µg/mL respectively) showed the assay to be fit for use (see supplementary data; S1). The drug was thought to be chemically unstable (Singh et al., 2013) and this was confirmed in this study (see supplementary data; S2), because a range of previously published work has failed to mention this issue (Pandey and Khuller, 2005; Pandey et al., 2003; Zahoor et al., 2005).

2.6. Nanocarrier loading

For lipid shell nanocarriers, rifampicin was incorporated into the carriers by dissolving the drug in 2 mL of acetone and then adding the mixture to the triglyceride. The acetone was removed by evaporation before continuing with the manufacture protocol. In order to try and enhance the interaction between rifampicin and oil, several batches of nanocarriers were produced containing the ion-pairing counterions, sodium stearate and sodium ethyl acetate in the oil core. The counterions were combined with rifampicin at the molar ratio of 1:20 during the manufacture. For the fabrication of drug loaded PVA shell nanocarriers, 15 mg of rifampicin was dissolved in the organic phase and the manufacture was repeated as previous protocol.

An Amicon centrifugal device was used to determine the loading efficiency. The amount of drug contained in a) the purified suspension as a whole, b) the nanocarriers only and c) the continuous phase was assayed. The nanocarriers were separated from the continuous phase using Amicon ultra 0.5 centrifugal filter devices with ultracel 100 membranes (100 kDa molecular weight cut off) (Millipore, UK). Aliquots of 0.5 mL were removed from the purified nanocarrier suspension and placed in the sample reservoir of the filter devices and centrifuged for 30 min at 14,000 *g* at ambient temperature (Biofuge Pico centrifuge, Heraeus, Buckinghamshire, UK). During this process any free drug in the

continuous phase passed through the filter into the receiver chamber, and the drug loaded nanocarriers were retained on the filter. The filtrate was diluted with water and subjected to HPLC analysis and the nanocarriers were dissolved in methanol and subjected to HPLC analysis. The drug recovery and loading efficiency of the purified nanocarrier suspensions were calculated according to equations [1] and [2]:

$$\text{Drug recovery} = \frac{\text{Mnanocarrier + Mfiltrate}}{\text{Msuspension}} \quad [1]$$

$$\text{Loading efficiency (\%)} = \frac{\text{Mnanocarrier}}{\text{Minput}} \quad [2]$$

Where $M_{suspension}$ was the mass of drug in the nanocarrier suspension; $M_{nanocarrier}$ was the mass of drug encapsulated into the nanocarrier; $M_{filtrate}$ was the mass of drug in aqueous filtrate and M_{input} was the mass of drug added during manufacture.

2.7. Release of rifampicin from the nanocarriers

To characterize rifampicin release from the lipid shell nanocarriers, the drug remaining in the carriers with and without prior exposure to shell permeabiliser Pluronic L62D was measured. When the shell permeabliser was used it was mixed with the purified nanocarrier suspensions at a Pluronic: nanocarrier ratio of 1:0.5 w/w. The release of rifampicin from the lipid shell nanocarriers was determined by dialyzing the nanocarrier suspensions against 500 mL PBS buffer adjusted to pH 7.4 or 4.2 (1.6 mg nanocarrier per mL buffer) at 37°C. For the PVA shell nanocarriers the suspensions generated by the manufacture method were mixed with PBS pH 7.4 in a 1:1 v/v ratio at 37°C and the drug release was determined by dialysis. To permeabilise the PVA shell nanocarriers PBS buffer pH 4.2 was added to nanocarrier suspension in a 1:1 v/v for 1 min and then mixture was transferred to a dialysis bag and dialysed against 500 mL of PBS buffer (0.06 mg nanocarrier per mL buffer) at either pH 7.4 or pH 4.2 to determine the drug release. The rifampicin solubility was measured to be 1550 µg/mL at pH 7.4 and 750 µg/mL at pH 4.2, thus sink conditions were maintained in all the release experiments (total rifampicin loading per 500 mL was ca.1.2mg). To monitor the drug release from all the nanocarrier experiments 0.5 mL aliquots were removed from dialysis tubing containing the suspensions (12-14 kDa molecular weight cut off) at a series of pre-determined time points and rifampicin content in the

nanocarriers was measured by HPLC (as detailed in the loading assessment method). The drug content remaining in the nanocarriers was calculated according to equation [3]:

$$\text{Release } (\%) = \frac{M0 - Mt}{M0} [3]$$

Where$M_0$was the mass of drug in nanocarrier at t_0 and M_t was the mass of drug in nanocarrier at a time point. The drug remaining in both the PVA polymer and lipid shell nanocarriers was quantified rather than the drug released into the dialysis solution as previous reports had suggested that rifampicin was chemically unstable in aqueous solution (Singh et al., 2000).

2.8. Shell permeabiliser induced changes of the lipid nanocarriers

Changes in the size of the lipid nanocarries in response the shell permeabiliser were measured after the suspensions were exposed to Pluronic surfactant using identical conditions as in the release study. At regular intervals between 30 min and 24 h post permeabiliser exposure samples were taken from the dialysis tubing where the particles were being suspended and the particle size was measured. PCS was also used to study the effect of pH on the ability of surfactant to aggregate. Surfactant solutions of 1 to 100 mg/mL were prepared in PBS at the two pHs7.4 and 4.2 as used in the release study. The derived count rate of the solutions were measured and the critical micelle concentration (CMC) of the surfactant in each of the pH conditions was determined by estimating where the two linear models applied to the derived count rate data intercepted. The lipid shell nanocarriers were also visualised using Transmission electron microscopy (TEM) before and after exposure to the shell permeabiliser. The suspension (3 μL) was applied to a Pioloform-coated copper grid and allowed to settle for one min. Excess suspension was blotted away with filter paper and the grid washed twice over distilled water before negative staining with 3 μL of an aqueous 1% uranyl acetate solution. The grids were allowed to dry before examination with a Tecnai T12 electron microscope (FEI, Oregon, USA).

2.9. Polymer nanocarrier changes induced by the shell permeabiliser

The particle size of the polymer shell nanocarriers had been previously determined not to change in preliminary work (data not shown) and hence changes in the chemical composition of the carrier matrix upon exposure to the shell permeabiliser were characterised

using Fourier transform infrared spectroscopy (FTIR) (Perkin Elmer, Beaconsfield, UK). The FTIR spectrometer was fitted with a DuraSamplIRII diamond attenuated total reflectance attachment (Smiths detection, Warrington, UK). Each sample was applied in its liquid state to the diamond and 32 scans were performed to generate the spectra. Peak positions were determined using Spectrum One software (version 6).Intensities of peaks referring to O-H and C-O bonds were specifically analysed in order to search for changes in the polymer hydrolysis over time. Nanocarrier size change before and after the shell permeabliser were captured by TEM as described above.

2.10. Statistical analysis

SPSS version 20 (IBM, UK) was used for all statistical analyses. The normality (Sapiro-Wilk) and homogeneity of variances (Levene's test) of the data were assessed prior to statistical analysis. The release data were analysed statistically using T-test or Mann-Whitney test. Differences were considered to be statistically significant at a level of $P < 0.05$.

3. Results and discussion

3.1. Nanocarrier characterisation

Polyvinyl acetate was saponified to produce PVA, which was determined to be 32% hydrolysed by NMR analysis (see supplementary data; S3). This PVA was used to manufacture the polymer shell nanocarriers. PCS size analysis of the purified polymer nanocarrier suspensions revealed a unimodal, normally distributed particle population in the nanometre size range (see supplementary data; S4). The blank lipid shell nanocarriers and the polymer shell nanocarriers had a mean diameter of ca. 50 and 250 nm and a polydispersity index of 0.074 ± 0.02 and 0.143 ± 0.02, respectively (Table 1). The lipid shell nanocarriers possessed a zeta potential of -3.46 ± 0.60 mV whilst the polymer shell nanocarriers had a zeta potential of-0.27 ± 0.45mV. In order to investigate whether the dispersion medium was having a significant influence on the PCS data, the particle size measurements were repeated upon serial dilution of the nanocarrier suspensions. The size measured upon dilution was consistent for the lipid shell nanocarriers over the tested dilution range, the effective diameter, i.e. the predicted size at infinite dilution was 49 nm (see supplementary data; S5). However, the size of the polymer shell nanocarriers reduced in size upon dilution due to the interference of the water soluble stabiliser with the size measurements, hence it gave an effective

hydrodynamic diameter of 204 nm (see supplementary data; S5). The size and polydispersity of the nanocarriers employed in this work were consistent with those previously reported using similar preparation methods (Chana et al., 2015; Madlova et al., 2009). The emulsion-precipitation method of nanocarrier fabrication was shown to generate a much higher nanocarrier solid content compared to the injection-precipitation method (Table 1).

Table 1: Size, polydispersity, zeta potential and solid content for non-loaded (blank) and rifampicin-loaded lipid nanocarriers (LNC) and poly(vinyl alcohol) (PVA) polymer nanocarriers. *Measured at a nanocarrier concentration of 80 mg/mL and 3 mg/mL for lipid and polymer nanocarriers respectively. Data represent mean ± standard deviation (n = 3).

Nanocarrier type	**Mean size* (nm)**	**Polydispersity* index**	**Zeta potential*(mV)**	**Solid content (mg/mL)**
LNC_{blank}	52 ± 2	0.07 ± 0.02	-3.46 ± 0.60	146.7 ± 12.2
$LNC_{rifampicin}$	50 ± 3	0.07 ± 0.02	-2.07 ± 0.62	163.3 ± 7.0
PVA_{blank}	249 ± 5	0.14 ± 0.02	-0.27 ± 0.45	5.9 ± 1.5
$PVA_{rifampicin}$	261 ± 7	0.22 ± 0.02	-0.26 ± 0.37	6.0 ± 0.9

3.2. Lipid nanocarrier drug release

Rifampicin loaded into the lipid nanocarriers with a loading efficiency, 41.0 ± 11.4%. Drug recovery (mass balance) in the loading determinations was >90%. Continuous passive release from the lipid nanocarriers was observed over 24 h at both pH 7.4 (A) and pH 4.2 (C) (Fig.1). This continuous release, which presumably commenced immediately after manufacture, required the release testing be performed at an identical time post manufacture in all the studies. This strategy led to acceptable intra-batch variability across the experiments. Attempts to reduce the passive drug release, using an ion-pairing strategy to retain the drug in the oil, were unsuccessful (Fig.2). Ion-pairing was employed in this work because it has been used previously to improve the retention of hydrophilic drugs in a lipid matrix nanocarrier (Zhao et al., 2016) and it has been shown to modify drug release kinetics without changing the chemical structure of the drug (Song et al., 2016). However, this strategy has not been previously applied to modify the drug release of rifampicin from nanocarriers. Theoretically, rifampicin and the counterions are fully ionized in acidic conditions enabling ion-pairs to form during the nanocarrier manufacturing process. In addition, the hydrophobicity of the complex should increase as the counterions (log P: ethyl acetate 0.28, stearate 3.62, calculated by Marvin Sketch, ChenAxon Ltd, Hungary) should

produce an ion-paired complex with reduced polarity compared to the parent drug and greater affinity for lipid nanocarrier oil core. Therefore, the inability of the counterions used in this work to slow rifampicin diffusion out of the nanocarriers was thought to be because rifampicin did not effectively form ion pairs in the nanocarrier. This may have been because the drug localised at the oil core-nanocapsule shell interface whereas the counterions located in the oil core, or because steric hindrance arising from the molecular structure incompatibility that prevented ion-pair formation.

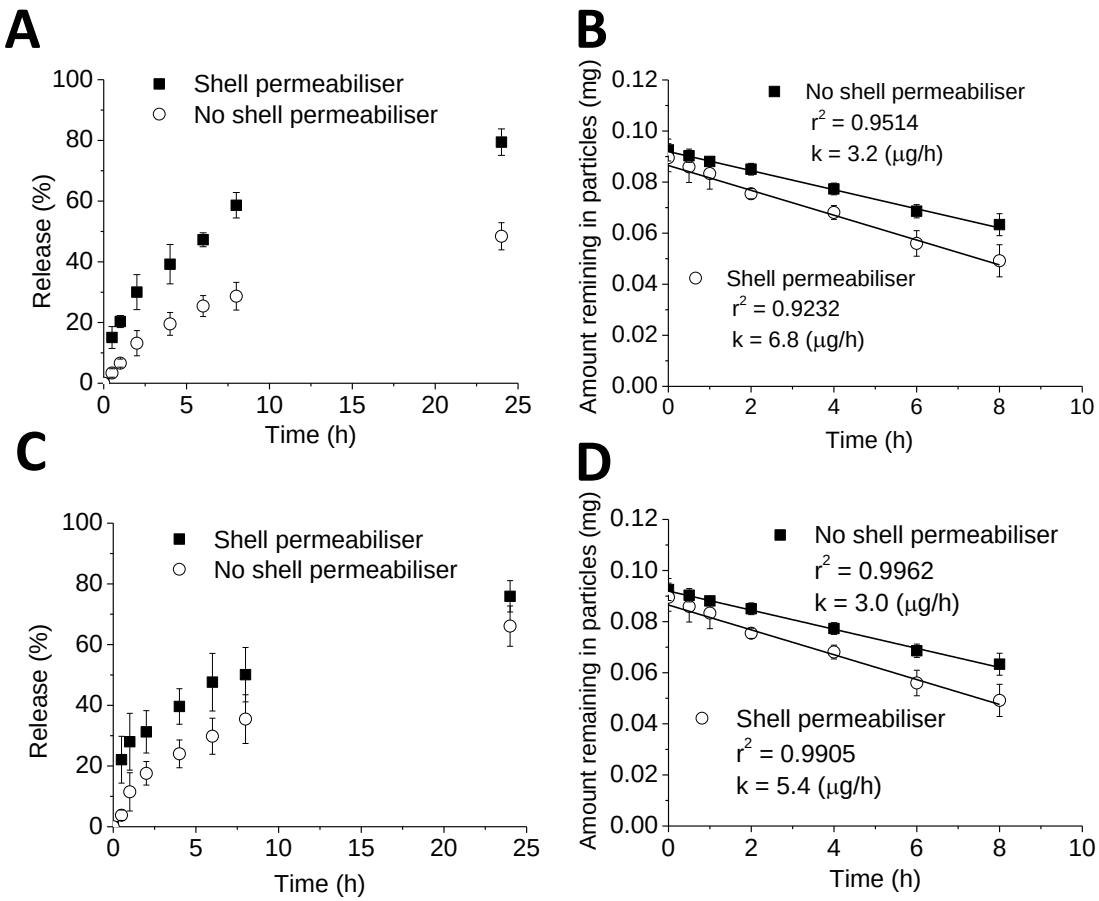

Fig.1.Percentage drug release of rifampicin from the lipid nanocarriers with and without the co-administration of the shell permeabiliser, Pluronic L62D 1:0.5 w/w, in (A) PBS buffer pH 7.4 and (C) PBS buffer pH 4.2. Graph (B) and (D) show the corresponding amount of rifampicin within the particles versus time fitted with a linear model. Data represent mean ± standard deviation (n = 3).

Although an inherent continuous drug release from the control lipid nanocarriers occurred, i.e., without the addition of the permeabiliser, there was still a significant increase in the extent of release at each time point when the shell permeabilisers were added to the nanocarriers at pH 7.4 ($P<0.05$). The drug release rate (k) for the lipid nanocarrier in the

presence of the shell permeabiliser was double that of the control system ($P<0.05$), with the control and permeabilised nanocarriers releasing approximate 50% and 80% of their rifampicin load over 24 h. At pH 4.2 the significant difference in release rate ($P<0.05$) when the permeabilised and non-permeabilised nanocarrier test systems were compared was still evident. The rate of drug release from the control nanocarriers at pH 4.2 and pH 7.4 was very similar at 3.2 µg/h and 3.0 µg/h respectively despite the lower aqueous solubility of rifampicin at pH 4.2 (0.75 mg/mL). This signified that the lipid shell was exerting a good degree of control over fluid ingress and drug release.

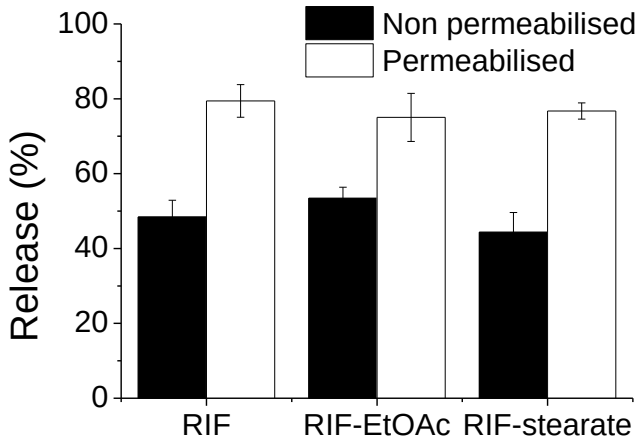

Fig.2. Rifampicin (RIF) release from lipid nanocarriers after 24 h in phosphate buffered saline at pH 7.4 when rifampicin was formulated as the base or ion paired with ethyl acetate (EtOAc) or stearate. Permeabilised lipid nanocarriers release was achieved by the addition of PluronicL62D.Data represent mean ± standard deviation (n = 3).

Regardless of whether or not the nanocarrier shells were permeabilised, the lipid nanocarrier drug release showed zero order kinetics (Fig 1 B, D) and this matched previous reports of drug release from lipidic nanomaterials (Abdel-Mottaleb et al., 2010; Zhai et al., 2014). Zero-order release suggested that rifampicin was encapsulated by the lipid shell of the nanocarrier. However, the release of rifampicin was much more higher compared to that previously reported (< 5% release after 24 h) for rhodamine using the same carrier system (Chana et al., 2015). The difference in the release profiles was most probably driven by the different physicochemical properties of the nanocarrier payloads. Rifampicin has pKas of 1.7 and 7.9 and a Log P of 1.1(Bhise et al., 2010) whereas rhodamine has a pKa of 4.2 and log P of 2.7 (Lahnstein et al., 2008), hence rhodamine should naturally display a higher affinity to the oil core of the nanocarriers.

Although a continuous release from the lipid shell nanocarrier was observed, there was no initial burst release. There is not a standard method that is used to determine burst release from nanocarriers, so in this study the % of drug release at t=0.5 h was used as a measure of bust release. The lipid shell nanocarriers showed a 5% release at t=0.5 h, whereas previous studies using nanocarriers typically cite an initial release of up to 30-40% when reporting problems with burst release (Nayak et al., 2010).

3.3. Polymer shell nanocarrier drug release

The drug loading in the polymer shell nanocarrier was 25.9 ± 2.3%. At pH 7.4 continuous drug release (k=2.3 μg/h) was observed, which was enhanced upon exposure to the shell permeabiliser (k=3.4 μg/h) ($P<0.05$, Fig.3). At 0.5 h a 10% release was recorded, which was much lower than previous reports of up 80% burst release over a similar time frame with a polymer nanocarriers (Sabzevari et al., 2013). Almost 80% of drug came out the polymer nanocarriers, which were subject to permeabilisation over 8 h, this was nearly double the non-permeabilised system ($P<0.05$). When the release study was repeated in the pH 4.2 medium similar profiles were observed with and without the permeabiliser. There was no significant difference in k across the two different pH experiments for the nanocarriers in the absence of the shell permeabilisers ($P>0.05$, Fig.3).

Several new polymeric nanoparticle technologies have been investigated recently for drug delivery applications. These include porous nanoparticle-aggregate particles, dynamic pH responsive nanoparticles and self-assembling nanoparticles, but the use of these systems in pharmaceutical products has been limited by scale up and toxicity concerns (Kean and Thanou, 2010). PVA is a water soluble synthetic polymer that is formed by full or partial hydrolysis of poly(vinyl acetate) (PVAc). PVA has proven to be safe as a coating agent for pharmaceutical and dietary supplement products, it has good compatibility with lung cells and in comparison to other polymeric systems it has a limited potential to cause local lung inflammation (DeMerlis and Schoneker, 2003). Furthermore, the production of the nanocarriers using PVA is easily scalable. Therefore, this material is well suited to the formation of nanocarriers for clinical applications (Madlova et al., 2009). The amphiphilic grades of the polymer (30–60% hydrolysis), are the most interesting in terms of drug delivery due to their biocompatibility and amphiphilic properties, but they are not readily available. Therefore, PVA was synthesised in this study to attain a degree of hydrolysis that would

spontaneously generate nanocarriers in an aqueous solution (Chana et al., 2008; Madlova et al., 2009).

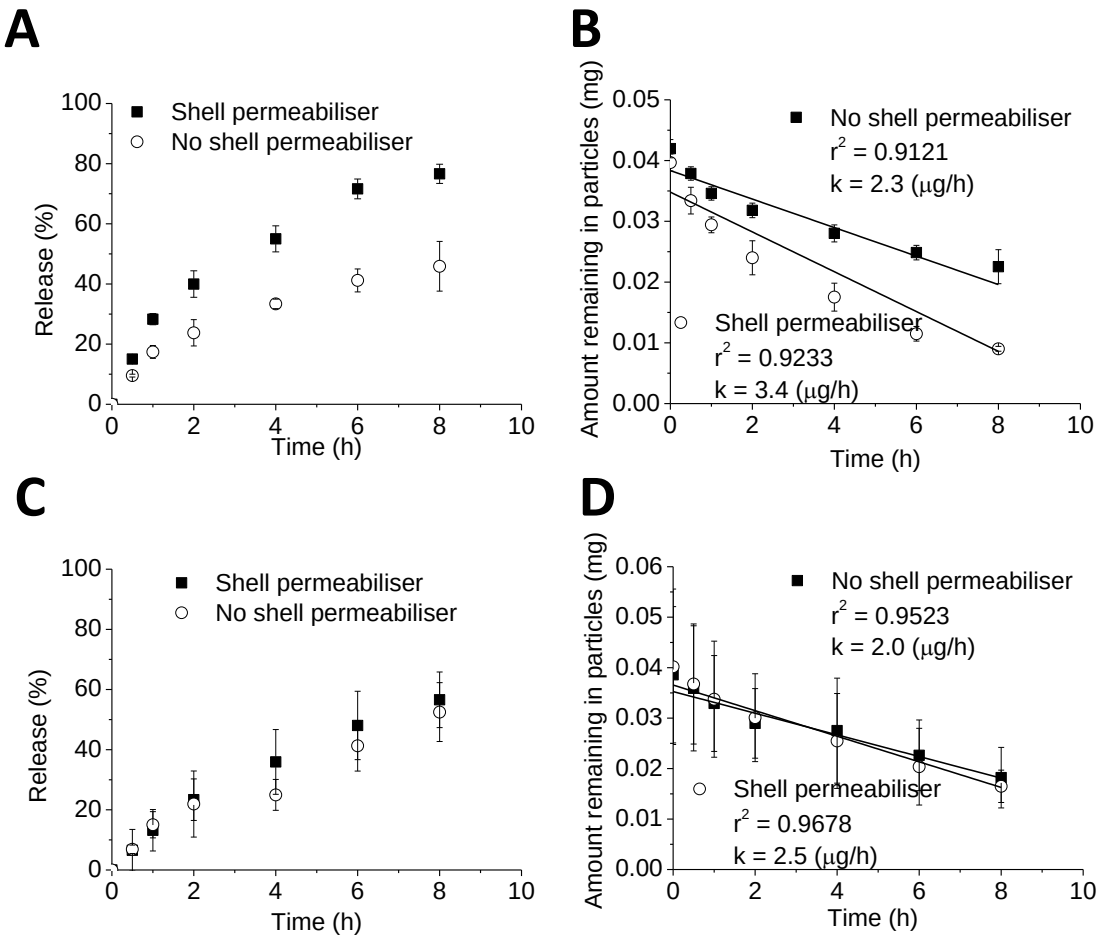

Fig.3. Release of rifampicin from polymer shell nanocarriers in (A) PBS buffer pH 7.4 and (C) PBS buffer pH 4.2.Graph (B) and (D) show the application of a linear model to the drug release data. Data were shown as mean ± standard deviation (n = 3).

It is generally assumed that the main release process from polymeric nanocarriers is diffusion through the polymer matrix, but release can also be facilitated by polymer degradation (Soppimath et al., 2001). In the case of the polymer nanocarriers in this work the drug is placed in an oil core that is coated with the polymer and therefore the release from the carrier requires diffusion of the drug through the polymeric shell. This mechanism is consistent with the zero-order kinetics observed in this study.

It was unexpected that at pH 4.2 medium, the rate of drug release was not enhanced by the permeabiliser. This result suggested that another factor was confounding the enhanced drug release at this acidic pH. The lower aqueous solubility at pH 4.2 compared to pH 7.4

could have been one factor responsible for different release characteristics at the more acidic pH. However, the fact that this pH dependant change in solubility appeared to influence the release from the polymer systems more that the lipid system also suggested that perhaps the polymer nanocarriers were more susceptible to water ingress compared to the lipid shell carriers.

3.4. Permeabilisation mechanism for lipid shell nanocarriers

The exposure of lipid shell nanocarriers to the Pluronic surfactant permeabiliser at pH 7.4 induced a substantial increase in the carrier size over time ($P<0.05$), resulting in a mean size of 240 ± 1 nm at 24 h (Fig.4). TEM images of control lipid nanocarrier suspensions revealed the presence of spherical particles in the 50 nm size range (Fig.5). Following an 8 hour exposure to Pluronic L62D at pH 7.4 the lipid shell nanocarriers were larger (~200 nm), which agreed with the light scattering data (Fig.4). This nanocarrier permeabilisation process at pH 7.4 was similar to that previous work (Chana et al., 2015). However, previously the size changes of the lipid nanocarriers in acidic dissolution media had not been reported and this study showed that no size change occurred at pH 4.2 compared to control nanocarriers. The light scattering data revealed that the Pluronic L62D surfactant displayed a significantly lower CMC (8.1 ± 1.4) at pH 4.2 compared to pH 7.4 (25.2 ± 2.1) (Fig.4) ($P<0.05$), indicating the greater propensity for the surfactant to aggregate in the more acidic pH medium, thus a lower propensity to interact with the nanocarriers.

For Pluronics with intermediate PO block lengths, such as the grade used in this study, insertion into bilayers is the primary means of membrane interaction. The external semisolid shell of the lipid nanocarriers was composed of phospholipid, thus Pluronic was expected to interact with the shell in a similar manner to a lipid bi-layer, i.e., inserting into the later with the two EO segments of the surfactant residing on the apical side of the membrane and the PO chain protruding into the hydrophobic domain (Firestone et al., 2003). The pH-dependent swelling responses to Pluronic L62D supported the shell insertion mechanism of action because the increased propensity for the PEO-PPO-PEO block copolymer to aggregate in the aqueous solution would diminish its affinity for the nanocarrier shell surface (Mao et al., 2001). Although previous work has shown that the Pluronic PEO block can be degraded in strong acids, at pH 4.2, this effect was not expected to be as significant as the change in CMC demonstrated using the light scattering data (Yang et al., 2006).

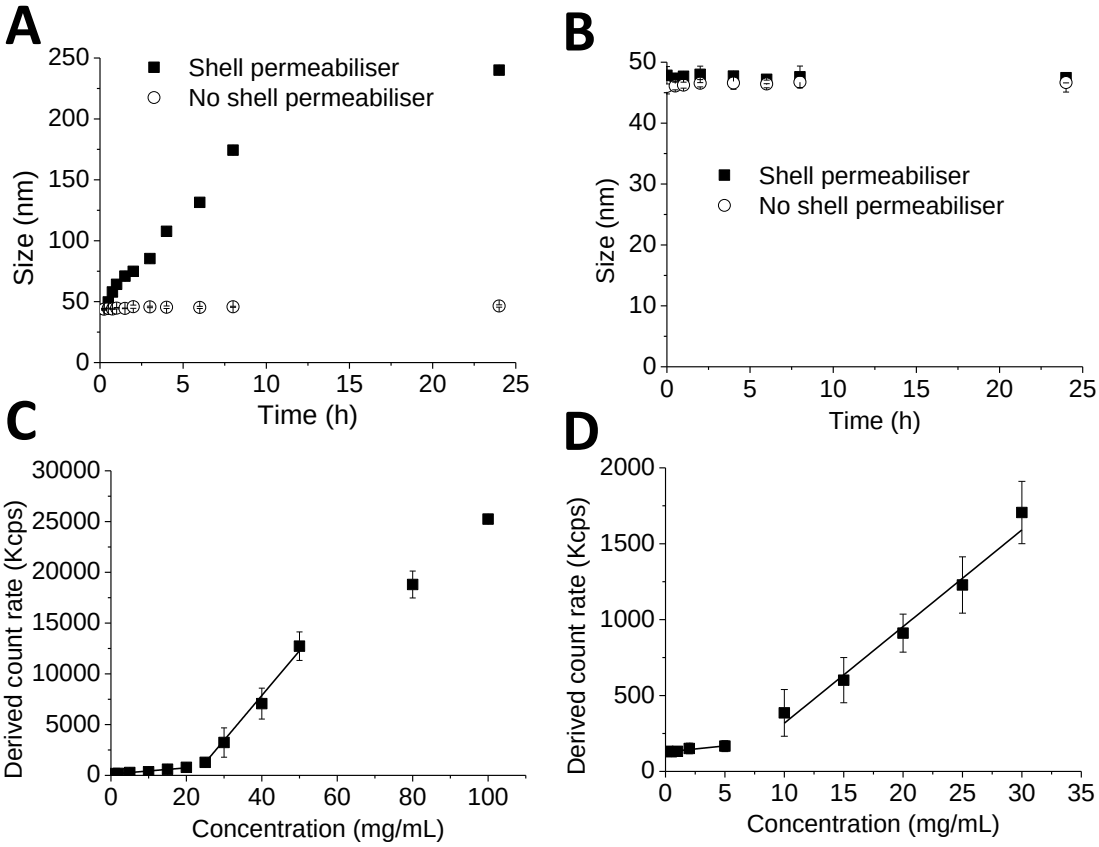

Fig.4. Lipid nanocarrier distension over time following exposure to the shell permeabiliser Pluronic L62D at (A) pH 7.4 and (B) 4.2.Critical micelle concentration (CMC) of Pluronic L62D at (C) pH 7.4 and (D) 4.2.Data represent mean ± standard deviation (n = 3).

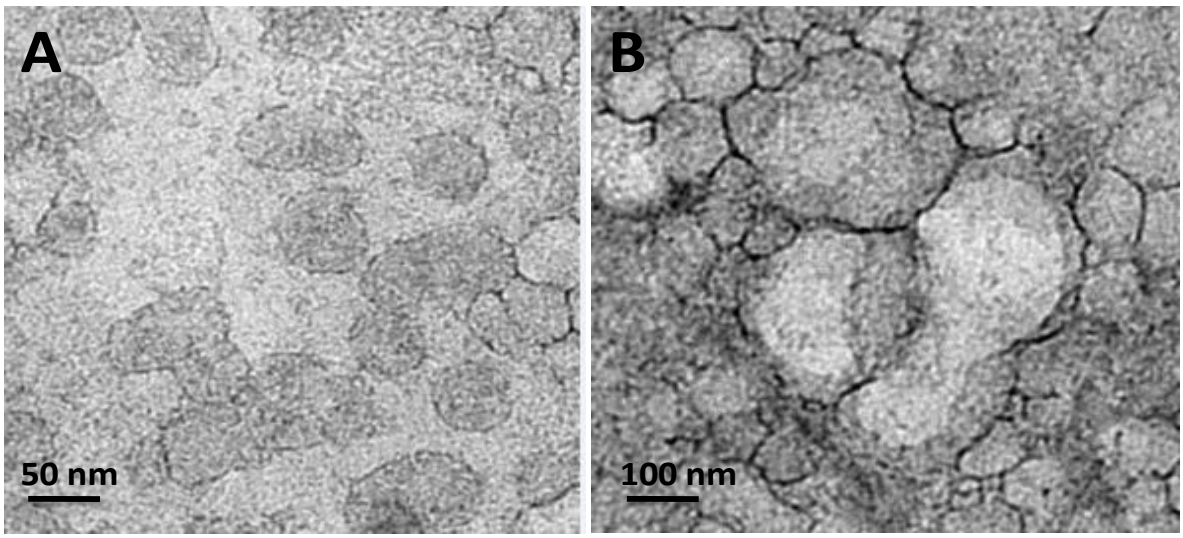

Fig.5. Transmission electron microscopy (TEM) images of lipid shell nanocarrier suspensions (A) before exposure to Pluronic L62D surfactant (80 mg/mL), (B) 8 h after exposure to the Pluronic L62D surfactant at pH 7.4.

3.5. Permeabilisation mechanism for the polymer shell nanocarriers

FTIR chemical analysis of the polymer shell nanocarriers showed that there was no difference in the intensity of OH peak over time when they were not exposed to the shell permeabiliser (Fig.6), which suggested the polymer's structure was unchanged. For the nanocarrier exposed to the shell permeabilising acidic conditions, the intensity of hydroxyl group increased over time. TEM showed that the shell permeabliser had no effect on particle sizeor the ingress of stain to the nanocapsule core as illustrated in Fig.7. These results suggest the mechanism of permeablisation in this dynamic nanosystem was polymer modification via carboxyl functional group hydrolysis caused by the acidic conditions.

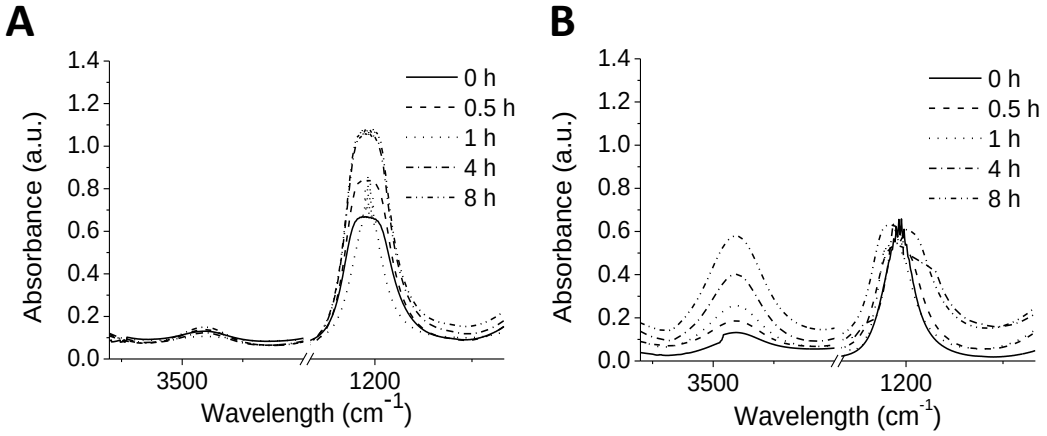

Fig.6. FTIR spectra for polymer shell nanocarriers permeabilised by (A) buffer pH 7.4 and (B) buffer pH 4.2. Regions of interest were the OH stretching region (3700-3200 cm^{-1}) and the C-O stretching region (1200-1000 cm^{-1}).

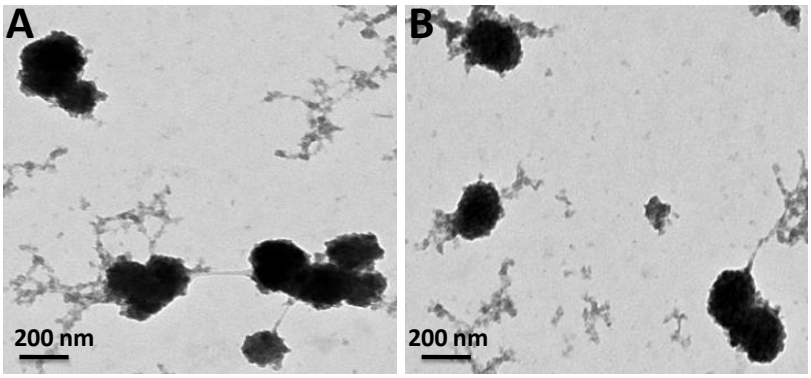

Fig.7.Transmission electron microscopy (TEM) images of (A) non non-permeabilisedpolymer shell nanocarriers and (B) polymer nanocarriers permeabilised by the addition of an acid solution.

It is well known that ester group of PVA can be hydrolysed to an alcohol under acidic conditions (Clayden et al., 2012). Increasing the amount of hydroxyl groups would enhance the affinity of the polymer membrane to water and increase surface film solvation, which would facilitate drug release via diffusion through membrane pores. The acid solution induced the polymer hydrolysis within 1 h, which was similar to the time frame of polymer hydrolysis used to generate the polymers. It is also possible that the polymers molecular weight can be reduced due to hydrolysis which could facilitate drug release (Xu and Du, 2003). However, in the time frame of the release experiments it was thought that an increase PVA film hydration was most probably the primary cause of the increase in drug release because the kinetics of polymer degradation is much slower than that of the hydrolysis reaction. The fact that the polymer was hydrolysed upon incubation in a pH 4.2 solution supported the notion that the lower aqueous drug solubility at pH 4.2 compared to pH 7.4 was responsible for inability for the permeabiliser to improve drug release at the acidic pH rather than any effects elicited by the nanocarrier structure.

4. Conclusions

Rifampicin loaded lipid shell nanocarriers and polymer shell nanocarriers both provided controlled zero order drug release. The carriers controlled release primarily through their outer shells. As a consequence, when the nanocarrier shells were permeabilised greater quantities of drug diffused out of the carriers. The lipid nanocarriers were permeabilised using a Pluronic surfactant, which inserted into the outer shell, whereas the polymer carriers were permeabilised through polymer hydrolysis. Both these release mechanisms were effective in an environment at 7.4, but at pH 4.2the permeabilisation was only effective for lipid nanocarriers. The loading capacity and their ability to increase in size, which could improve macrophage targeting, and their ability to have their drug release manipulated by shell permeabilisers at pH 4.2 and pH 7.4renders the lipid nanocarriers a very interesting system to facilitate drug delivery to the lung.

References

Abdel-Mottaleb, M.M., Neumann, D., Lamprecht, A., 2010. In vitro drug release mechanism from lipid nanocapsules (LNC). Int. J. Pharm. 390, 208-213.

Bhise, S.B., More, A.B., Malayandi, R., 2010. Formulation and in vitro evaluation of rifampicin loaded porous microspheres. Sci. Pharm. 78, 291.

Chana, J., Forbes, B., Jones, S.A., 2008. The synthesis of high molecular weight partially hydrolysed poly (vinyl alcohol) grades suitable for nanoparticle fabrication. J. Nanosci. Nanotechnol. 8, 5739-5747.

Chana, J., Forbes, B., Jones, S.A., 2015. Triggered-release nanocapsules for drug delivery to the lungs. Nanomed. Nanotechnol. Biol. Med. 11, 89-97.

Clayden, J., Greeves, N., Warren, S., 2012. Organic Chemistry. 2nd. Oxford University Press. UK.

Danhier, F., Lecouturier, N., Vroman, B., Jérôme, C., Marchand-Brynaert, J., Feron, O., Préat, V., 2009. Paclitaxel-loaded PEGylated PLGA-based nanoparticles: in vitro and in vivo evaluation. J. Control. Release. 133, 11-17.

DeMerlis, C., Schoneker, D., 2003. Review of the oral toxicity of polyvinyl alcohol (PVA). Food Chem. Toxicol. 41, 319-326.

Firestone, M.A., Wolf, A.C., Seifert, S., 2003. Small-angle X-ray scattering study of the interaction of poly (ethylene oxide)-b-poly (propylene oxide)-b-poly (ethylene oxide) triblock copolymers with lipid bilayers. Biomacromolecules 4, 1539-1549.

Ganta, S., Devalapally, H., Shahiwala, A., Amiji, M., 2008. A review of stimuli-responsive nanocarriers for drug and gene delivery. J. Control. Release. 126, 187-204.

Heurtault, B., Saulnier, P., Pech, B., Proust, J.-E., Benoit, J.-P., 2002. A novel phase inversion-based process for the preparation of lipid nanocarriers. Pharm. Res. 19, 875-880.

Holmkvist, A.D., Friberg, A., Nilsson, U.J., Schouenborg, J., 2016. Hydrophobic ion pairing of a minocycline/Ca 2+/AOT complex for preparation of drug-loaded PLGA nanoparticles with improved sustained release. Int. J. Pharm. 499, 351-357.

Janes, K.A., Fresneau, M.P., Marazuela, A., Fabra, A., Alonso, M.a.J., 2001. Chitosan nanoparticles as delivery systems for doxorubicin. J. Control. Release. 73, 255-267.

Jones, M.-C., Jones, S.A., Riffo-Vasquez, Y., Spina, D., Hoffman, E., Morgan, A., Patel, A., Page, C., Forbes, B., Dailey, L.A., 2014. Quantitative assessment of nanoparticle surface hydrophobicity and its influence on pulmonary biocompatibility. J. Control. Release. 183, 94-104.

Kean, T., Thanou, M., 2010. Biodegradation, biodistribution and toxicity of chitosan. Adv. Drug Delivery Rev. 62, 3-11.

Lahnstein, K., Schmehl, T., Rüsch, U., Rieger, M., Seeger, W., Gessler, T., 2008. Pulmonary absorption of aerosolized fluorescent markers in the isolated rabbit lung. Int. J. Pharm. 351, 158-164.

Madlova, M., Jones, S., Zwerschke, I., Ma, Y., Hider, R., Forbes, B., 2009. Poly (vinyl alcohol) nanoparticle stability in biological media and uptake in respiratory epithelial cell layers in vitro. Eur. J. Pharm. Biopharm. 72, 438-443.

Mao, G., Sukumaran, S., Beaucage, G., Saboungi, M.-L., Thiyagarajan, P., 2001. PEO-PPO-PEO block copolymer micelles in aqueous electrolyte solutions: Effect of carbonate anions and temperature on the micellar structure and interaction. Macromolecules 34, 552-558.

Mindell, J.A., 2012. Lysosomal Acidification Mechanisms. Annu. Rev. Physiol. 74, 69-86.

Mukherjee, B., Santra, K., Pattnaik, G., Ghosh, S., 2008. Preparation, characterization and in-vitro evaluation of sustained release protein-loaded nanoparticles based on biodegradable polymers. Int. J. Nanomed. 3, 487.

Mura, S., Nicolas, J., Couvreur, P., 2013. Stimuli-responsive nanocarriers for drug delivery. Nat. Mater. 12, 991-1003.

Natarajan, J.V., Nugraha, C., Ng, X.W., Venkatraman, S., 2014. Sustained-release from nanocarriers: a review. J. Control. Release. 193, 122-138.

Nayak, A.P., Tiyaboonchai, W., Patankar, S., Madhusudhan, B., Souto, E.B., 2010. Curcuminoids-loaded lipid nanoparticles: novel approach towards malaria treatment. Colloids Surf B Biointerfaces. 81, 263-273.

Ohashi, K., Kabasawa, T., Ozeki, T., Okada, H., 2009. One-step preparation of rifampicin/poly (lactic-co-glycolic acid) nanoparticle-containing mannitol microspheres using a four-fluid nozzle spray drier for inhalation therapy of tuberculosis. J. Control. Release. 135, 19-24.

Pandey, R., Khuller, G., 2005. Solid lipid particle-based inhalable sustained drug delivery system against experimental tuberculosis. Tuberculosis 85, 227-234.

Pandey, R., Sharma, A., Zahoor, A., Sharma, S., Khuller, G., Prasad, B., 2003. Poly (DL-lactide-co-glycolide) nanoparticle-based inhalable sustained drug delivery system for experimental tuberculosis. J. Antimicrob. Chemother. 52, 981-986.

Parveen, S., Misra, R., Sahoo, S.K., 2012. Nanoparticles: a boon to drug delivery, therapeutics, diagnostics and imaging. Nanomed. Nanotechnol. Biol. Med. 8, 147-166.

Peer, D., Karp, J.M., Hong, S., Farokhzad, O.C., Margalit, R., Langer, R., 2007. Nanocarriers as an emerging platform for cancer therapy. Nat. Nanotechnol. 2, 751-760.

Pinkerton, N.M., Grandeury, A., Fisch, A., Brozio, J.r., Riebesehl, B.U., Prud'homme, R.K., 2012. Formation of stable nanocarriers by in situ ion pairing during block-copolymer-directed rapid precipitation. Mol. Pharm. 10, 319-328.

Sabzevari, A., Adibkia, K., Hashemi, H., Hedayatfar, A., Mohsenzadeh, N., Atyabi, F., Ghahremani, M.H., Dinarvand, R., 2013. Polymeric triamcinolone acetonide nanoparticles as a new alternative in the treatment of uveitis: In vitro and in vivo studies. Eur. J. Pharm. Biopharm. 84, 63-71.

Singh, H., Bhandari, R., Kaur, I.P., 2013. Encapsulation of Rifampicin in a solid lipid nanoparticulate system to limit its degradation and interaction with Isoniazid at acidic pH. Int. J. Pharm. 446, 106-111.

Singh, S., Mariappan, T., Sharda, N., Singh, B., 2000. Degradation of rifampicin, isoniazid and pyrazinamide from prepared mixtures and marketed single and combination products under acid conditions. Pharm. Pharmacol. Commun. 6, 491-494.

Song, Y.H., Shin, E., Wang, H., Nolan, J., Low, S., Parsons, D., Zale, S., Ashton, S., Ashford, M., Ali, M., 2016. A novel in situ hydrophobic ion paring (HIP) formulation strategy for clinical product selection of a nanoparticle drug delivery system. J. Control. Release. 229, 106-119.

Soppimath, K.S., Aminabhavi, T.M., Kulkarni, A.R., Rudzinski, W.E., 2001. Biodegradable polymeric nanoparticles as drug delivery devices. J. Control. Release. 70, 1-20.

Sosnik, A., Carcaboso, Á.M., Glisoni, R.J., Moretton, M.A., Chiappetta, D.A., 2010. New old challenges in tuberculosis: potentially effective nanotechnologies in drug delivery. Adv. Drug Delivery Rev. 62, 547-559.

Wang, Y., Kho, K., Cheow, W.S., Hadinoto, K., 2012. A comparison between spray drying and spray freeze drying for dry powder inhaler formulation of drug-loaded lipid–polymer hybrid nanoparticles. Int. J. Pharm. 424, 98-106.

Xu, Y., Du, Y., 2003. Effect of molecular structure of chitosan on protein delivery properties of chitosan nanoparticles. Int. J. Pharm. 250, 215-226.

Yang, B., Guo, C., Chen, S., Ma, J., Wang, J., Liang, X., Zheng, L., Liu, H., 2006. Effect of acid on the aggregation of poly (ethylene oxide)-poly (propylene oxide)-poly (ethylene oxide) block copolymers. J. Phys. Chem. B. 110, 23068-23074.

Zahoor, A., Sharma, S., Khuller, G., 2005. Inhalable alginate nanoparticles as antitubercular drug carriers against experimental tuberculosis. Int. J. Antimicrob. Agents 26, 298-303.

Zhai, Y., Yang, X., Zhao, L., Wang, Z., Zhai, G., 2014. Lipid nanocapsules for transdermal delivery of ropivacaine: in vitro and in vivo evaluation. Int. J. Pharm. 471, 103-111.

Zhao, S., Li, N., Garamus, V.M., Handge, U.A., Liu, J., Zhang, R., Willumeit-Römer, R., Zou, A., 2016. Doxorubicin hydrochloride-oleic acid conjugate loaded nanostructured lipid carriers for tumor specific drug release. Colloids Surf B Biointerfaces. 145, 95-103.